Europhys. Lett., **73** (1), pp. 83–89 (2006)
DOI: 10.1209/epl/i2005-10356-y

Helical ground state and weak ferromagnetism in the edge-shared chain cuprate $NaCu_2O_2$

S.-L. Drechsler[1](*), J. Richter[2], A. A. Gippius[3], A. Vasiliev[3], A. A. Bush[4], A. S. Moskvin[5], J. Málek[6], Yu. Prots[7], W. Schnelle[7] and H. Rosner[7]

[1] *IFW Dresden - P.O. Box 270116, D-01171 Dresden, Germany*
[2] *Institut für Theoretische Physik, O.-v.-Guericke-Universität Magdeburg - Germany*
[3] *Moscow State University - Russia*
[4] *Moscow Institute of Radiotechnics, Electronics and Automation - Russia*
[5] *Ural State University - Ekaterinburg, Russia*
[6] *Institute of Physics ASCR - Prague, Czech Republic*
[7] *Max-Planck-Institut für Chemische Physik fester Stoffe - Dresden, Germany*

received 15 September 2005; accepted 26 October 2005
published online 2 December 2005

PACS. 74.72.Jt – Other cuprates, including Tl and Hg-based cuprates.
PACS. 76.60.-k – Nuclear magnetic resonance and relaxation.
PACS. 75.10.Pq – Spin chain models.

Abstract. – We report on susceptibility, magnetization, ^{23}Na NMR, and specific heat data of the spin-chain material $NaCu_2O_2$ in the paramagnetic and ordered phases. Below 13 K, where a sharp field-dependent specific heat peak appears, the NMR lineshape points to an incommensurate static modulation of the local magnetic field consistent with a spiral state of the Cu magnetic moments. At 2 K weak ferromagnetism with an ordered moment of about $4{\cdot}10^{-3}\mu_B$ has been observed. LDA-based estimates of exchange integrals reveal a large inchain frustration leading to a magnetic spiral.

Introduction. – Frustrated spin systems have attracted much attention during the last years (see, *e.g.*, ref. [1]). However, a particular challenging issue, coupled quantum (spin-1/2) chains with nearest-neighbor (NN) ferromagnetic (FM) and significantly strong next–nearest-neighbor (NNN) antiferromagnetic (AFM) inchain exchange have not been studied so far in detail. A searched physical realization has been found only recently in edge-shared cuprates $ACuO_2$ with divalent cations A = $[Li^+Cu^+]$, $[Na^+Cu^+]$, $[Li^+V^{+5}O_2^{-2}]$ [2–6]. These cuprates show Cu-O-Cu bond angles $\gamma \approx 94°$–$96°$ and incommensurate (IC) helical ground states with short quasi-periods and acute pitch angles ϕ [2, 5, 6]. Here, due to competing FM and AFM contributions the total NN exchange can be comparable or even smaller (in absolute value) than the AFM NNN one. Another often discussed scenario for helical-type order [7], usually for long quasi-periods (*i.e.* $\phi \ll 1$ or $2\pi - \phi \ll 1$), is provided by weak Dzyalozhinskii-Moriya (DM) exchange allowed for non-centrosymmetric crystals. The DM scenario allows also

(*) E-mail: drechsler@ifw-dresden.de

weak ferromagnetism absent in planar spirals. We will show that both scenarios, frustration and DM, are relevant in $NaCu_2O_2$. We report ^{23}Na nuclear magnetic resonance (NMR), magnetization, and specific heat data all indicating magnetic ordering below 13 K. The related phase can be ascribed to a spiral modulation of the magnetic moments consistent with the electronic and magnetic structure analyzed within local density approximation (LDA) and Hubbard models with a subsequent mapping on Heisenberg models. As a result, inchain frustration is found to drive the spiral order.

Structure. – $NaCu_2O_2$ crystals were grown similarly as described for the isomorphic $LiCu_2O_2$ [3, 6]. The analysis of the X-ray diffraction patterns recorded from single crystals and powdered single crystals at 300 K confirms that in contrast to $LiCu_2O_2$ our samples are *untwinned*, single-phased without any deviations from ideal occupancy parameters.

$NaCu_2O_2$ is orthorhombic with two copper sites: Cu^{2+} and Cu^{+}. There is less than 2% Na on Cu (probably Cu^{+}) sites. Hence, $NaCu_2O_2$ allows a more thorough study of the complex anisotropic properties and a refinement of the spiral structure. The lattice parameters $a = 6.210(2)$ Å, $b = 2.9369(5)$ Å, $c = 13.070(2)$ Å agree well with those in ref. [5] but differ considerably from the value of $c = 13.209$ Å given in ref. [8]. Anyhow, the LDA electronic structure is insensitive to these deviations. Edge-shared CuO_2 chains running along $\boldsymbol{b}$ form two bilayers shifted mutually by $b/2$ (fig. 1). Note that the ideal CuO_2 chain structure is distorted here: the central magnetically active Cu^{2+} ion is shifted off from the center of a CuO_4 plaquette by about 0.03 Å towards the NN chain. Hence, a center of inversion is lost. The broken local symmetry is reflected by different Cu-O-Cu bond angles $\gamma = 96°$ (inner) and $\gamma' = 94.7°$ (outer) ones. In addition, the CuO_4 plaquettes are tilted from the *ab*-plane by $\pm\phi_0 \approx \pm 4.2°$.

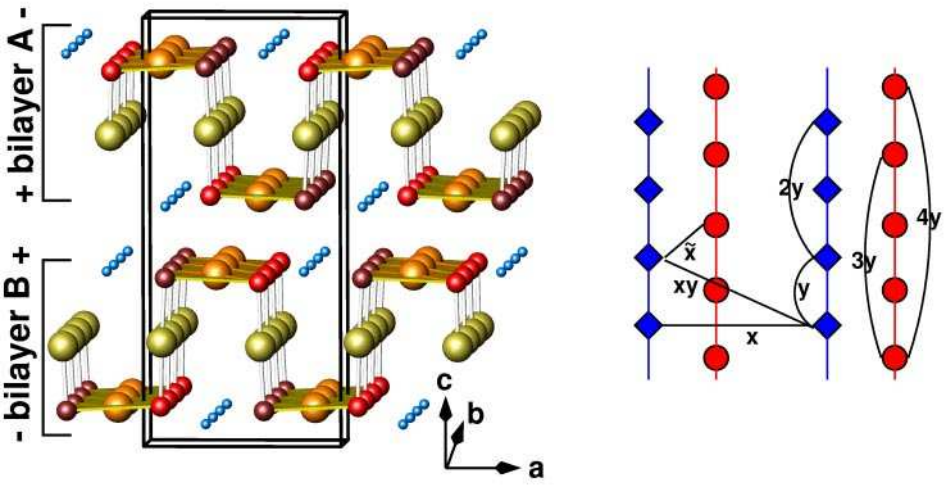

Fig. 1 – (Color on-line) Structure of $NaCu_2O_2$ (left). Upper (lower) half: bilayer A (B) with CuO_2 chains along $\boldsymbol{b}$. Cu^{2+}(orange), Cu^{+}(yellow), inner (outer) O (red (brown)), Na (blue) circles, respectively. Notice the staggered tilting $\pm$ of upper and lower chains within a bilayer. Schematical chain structure at the AB boundary with some exchange paths indicated (right). Filled diamond and circles denote CuO_4 plaquettes in B and A bilayers, respectively.

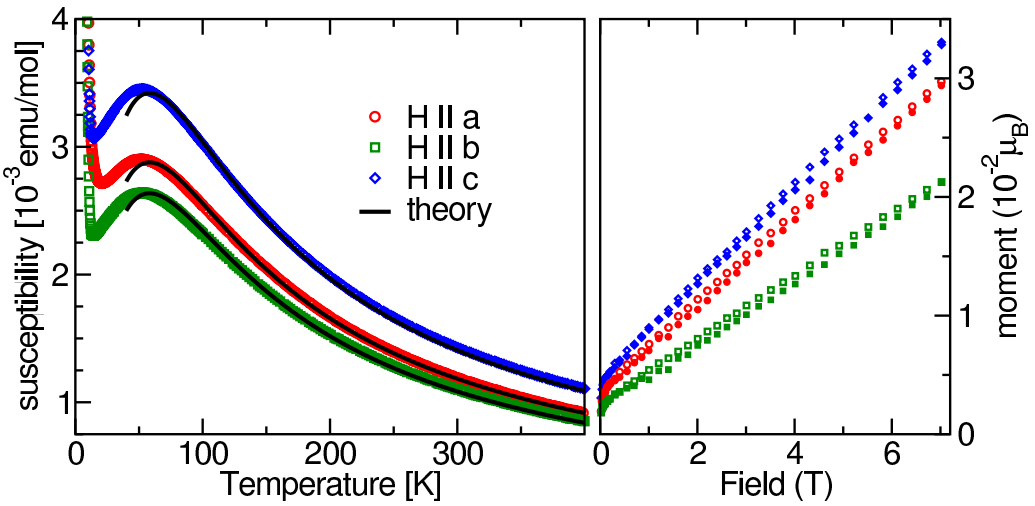

Fig. 2 – (Color on-line) Spin susceptibilities along the main crystallographic axes measured within magnetic fields $H = 0.1\,\mathrm{T}$ *vs.* temperature T. Theoretical curves for a periodic chain ($N = 16$ sites) with $J_1 = -4.09\,\mathrm{meV}$, $J_2 = 7.78\,\mathrm{meV}$ and anisotropic Landé-factors $g_c = 2.23$, $g_a = 2.05$, and $g_b = 1.96$; from top to bottom (left panel). The anisotropic magnetizations *vs.* H at $T = 2\,\mathrm{K}$ (right panel).

Experimental data and phenomenological analysis. – Microscopically, the magnetism of $NaCu_2O_2$ should be described by a general spin-1/2 Heisenberg-type model

$$\mathcal{H} = \sum_{ij,\alpha\beta} J_{ij}^{\alpha\beta} S_i^{\alpha} S_j^{\beta} + \vec{D}_{ij} \cdot (\vec{S}_i \times \vec{S}_j), \tag{1}$$

where i and j run over pairs of CuO_4 plaquettes. $\mathcal{H}$ exhibits a hierarchy of isotropic and anisotropic couplings with the leading terms given by isotropic NN and NNN inchain exchange. Indeed, the magnetic susceptibility $\chi(T)$ in the paraphase with $\boldsymbol{H} \parallel \boldsymbol{a}, \boldsymbol{b}, \boldsymbol{c}$ can be reasonably well described by the isotropic 1D J_1-J_2 model with $\alpha = -J_2/J_1 \approx 1.93$ (fig. 2) contrary to $\alpha \approx 5$ and sizable long-range exchanges J_3 and J_4 claimed in ref. [5]. We attribute this discrepancy mainly to a questionable subtraction of an "impurity ascribed low-T feature" (Curie law) which considerably affects a fit of $\chi(T)$ at $T < 50\,\mathrm{K}$. Anyhow, the negative curvature at low T and the shape of the $\chi(H)$ curves like in ref. [9] clearly show strong deviations from a Curie law. It is an *intrinsic* feature related to weak ferromagnetism emerging below $T^* \approx 8$–$9\,\mathrm{K}$. Its evidence stems from magnetization data obtained in external magnetic fields revealing signatures of a weak hysteresis and a small magnetic moment $M(T)$ at $T \to 0$ (fig. 2). For $T \leq 0.78T^*$ and $H = 0.1\,\mathrm{T}(\boldsymbol{H} \parallel \boldsymbol{a})$ a parabolic law

$$M(T) = M_0(1 - \eta(T/T^*)^2), \qquad \eta = 0.38, \qquad T^* = 8.3\,\mathrm{K}, \tag{2}$$

is obeyed such as for the classical weak ferromagnet $MnCO_3$ [10]. $M_0 \approx 4 \cdot 10^{-3}\mu_\mathrm{B}$ is a typical value in weak FM cuprates [9,11]. DM couplings explain naturally the weak ferromagnetism [10]. From the distortions discussed above we determine the orientation of the DM vectors $\boldsymbol{D}$ for NN and NNN spin pairs along $\boldsymbol{b}$ as $\perp$ to the local CuO_4 plaquette plane and tilted by $\pm\phi_0$ from $\boldsymbol{c}$ [12]. The $\boldsymbol{D}$ for i, j located at the AB bilayer boundary are tilted inphase. The nearly c-orientation of the main DM vectors explains the observed nearly ab-orientation of the helix. In a rigorous sense, we expect a more complex spin structure with

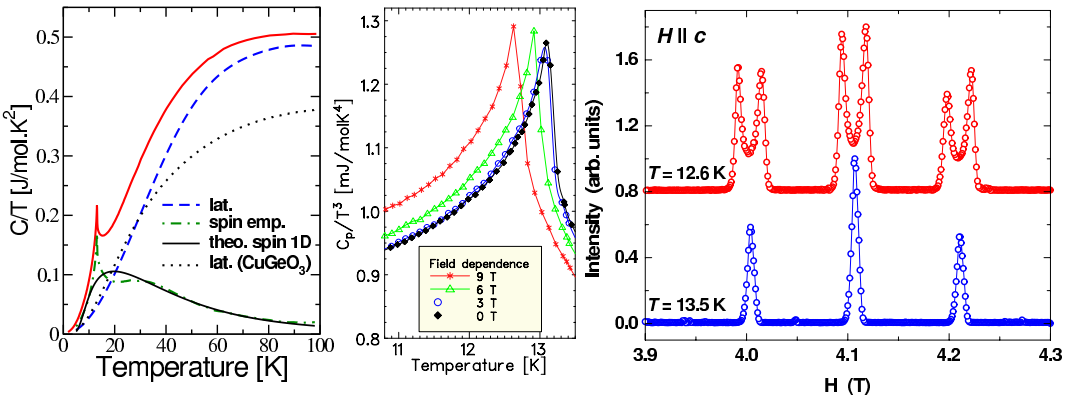

Fig. 3 – (Color on-line) Specific heat and NMR data. Total specific heat c_p and its contributions plotted as c/T *vs.* T (left panel). The experimental c_p (upper curve); the calculated 1D spin part $c_{\rm m}^{\rm th}$ from an $N = 16$ cluster (black thin curve) with J-values from $\chi(T)$-fits. The empirical lattice part $c_{\rm lat}^{\rm emp}$ (dashed curve) from (eq. (3)). The empirical 3D spin part (dash-dotted curve) from $c_{\rm m}^{\rm emp} = c_p - c_{\rm lat}^{\rm emp}$. For comparison the lattice part for $CuGeO_3$ (dotted curve) [22] is shown, too. The field dependence of c_p/T^3 *vs.* T (central panel). The ^{23}Na NMR spectrum below and above the magnetic phase transition at 13.1 K for $\boldsymbol{H} \parallel \boldsymbol{c}$ at 46.0 MHz (right panel).

two alternatingly tilted helices from each bilayer boundary. Using the fitted g_c and J_1 we estimate the NN DM vector as $\mid \boldsymbol{D}_1 \mid = (g_c - g)/g \mid J_1 \mid \sim 0.5\,$meV, where $g = (g_a + g_b + g_c)/3$.

Near $T_c = 13.1\,$K the specific heat c_p reveals a sharp peak and the ^{23}Na NMR spectra change dramatically, both signaling a phase transition (fig. 3). Without broadening the peak of c_p is nonlinearly shifted by -0.5 K by applying magnetic fields $\boldsymbol{H} \parallel \boldsymbol{c}$ up to 9 T: $T_c(H) \approx T_c(0)[1 - (H/H_0)^2]$, where $H_0 = 46.3\,$T. Thus, we attribute this peak to a magnetic phase transition. A broader feature has been reported near 12 K in ref. [5], however, we did not observe a shoulder near 7.5 K. The shoulder, the broader transition, and the lower T_c reported in ref. [5] might be due to significant disorder. Since, at variance with our work, a slight suppression (enhancement) of c_p below (above) T_c was reported for that polycrystalline sample [5], one might suggest *upward* shifts of T_c for $\boldsymbol{H} \parallel \boldsymbol{a}, \boldsymbol{b}$ and for improved polycrystalline samples [13]. The staggered tilting of CuO_4 plaquettes within a bilayer may cause oscillating terms in $\mathcal{H}$ and this way a staggered-field–induced magnetization which yields a spin gap Δ_s for one of the two acoustic branches near Γ, akin to the mechanism proposed for Cu-benzoate at the 1D Brillouin zone (BZ) boundary [14]. An H-dependent Δ_s could explain the field sensitivity of c_p at moderate H (fig. 3, central panel).

NMR spectroscopy being a local probe can be used to detect spin ordering. We report ^{23}Na NMR data of a $NaCu_2O_2$ single crystal. The spectra were measured for $\boldsymbol{H} \parallel \boldsymbol{c}$ by sweeping $\boldsymbol{H}$ at a fixed frequency of 32.2 MHz. The signal was obtained by integrating the spin-echo envelope. Above T_c a typical first-order quadrupole perturbed NMR spectrum for spin $I = 3/2$ was observed (fig. 3). The quadrupole splitting between the satellites in $NaCu_2O_2$ amounts to 196 mT, while in $LiCu_2O_2$ it is only 6 mT. The ratio is about 33, while the ratio of quadrupole moments $Q(^{23}\mathrm{Na})/Q(^{7}\mathrm{Li}) = 2.7$. Thus, the electrical-field gradient (EFG) at Na sites is much larger than that on Li in $LiCu_2O_2$. Note the dramatic change of the ^{23}Na NMR spectrum with asymmetric 1D van Hove singularity like peaks for $T < 13\,$K. The central transition line is characteristic for a IC modulation of the local magnetic field caused by a spin helix [15,16] of the Cu magnetic moments like in $LiCu_2O_2$ [3]. This is confirmed by similar lineshapes of

the satellite transitions, which in contrast to $LiCu_2O_2$ are here clearly observable due to the larger EFG and Q values given above. Noteworthy, the local magnetic field on Na(Li) sites estimated as the linewidth at the base of the central transition is only 80 mT (250 mT).

Turning to a phenomenological analysis of c_p, we have $c_p = c_{\rm m} + c_{\rm lat}$, to comprise the magnetic (spin) contribution $c_{\rm m}$ and the usual lattice part $c_{\rm lat}$. In first approximation we adopt again the 1D J_1-J_2 model with FM J_1 and AFM J_2 [17]. If $J_2 \gg -J_1$, $\mathcal{H}$ can be replaced by an effective Heisenberg model with a single AFM $J_{\rm eff} \approx J_2 + \beta J_1$, $\beta \ll 1$, in order to estimate the relevant temperature range. Using the Bethe-ansatz solutions [18] for $\chi(T)$ and $c_{\rm m}(T)$, from the maximum of the observed $\chi(T)$ near 50 K, $J_{\rm eff} \sim 80\,{\rm K}$ and a relevant temperature interval of about 160 K follows. In fact, using the J's which fit $\chi(T)$ for the calculated $c_{\rm m}$ a long tail extended up to about 200 K emerges. A straight empirical determination of $c_{\rm m}^{\rm emp}$ in this range is difficult since the phonon spectra of $NaCu_2O_2$ and $LiCu_2O_2$ are still unknown. However, at medium T an extended Debye approach can be used [19]:

$$c_{\rm lat}(T) \approx \beta_1 T^3 - \beta_2 T^5 + \beta_3 T^7 - \beta_4 T^9 + \beta_5 T^{11} \ldots . \tag{3}$$

We found a reasonable description for a broad range of temperatures $T \leq 95\,{\rm K}$ with $\beta_1 = 0.28\,{\rm mJ/mol{\cdot}K^4}$, $\beta_2 = 7.2{\cdot}10^{-8}\,{\rm J/mol{\cdot}K^6}$, $\beta_3 = 9.8{\cdot}10^{-12}\,{\rm J/mol{\cdot}K^8}$, $\beta_4 = 6.8{\cdot}10^{-15}\,{\rm J/mol{\cdot}K^{10}}$, and $\beta_5 = 1.9 \cdot 10^{-20}\,{\rm J/mol{\cdot}K^{12}}$. With this value of β_1 and 5 atoms per formula unit one arrives at a Debye temperature $\Theta_{\rm D}(T=0) = 326$ K. Similar numbers have been reported for other edge-shared cuprates such as $Sr_{0.73}CuO_2$, $Ca_{1-x}CuO_2$ ($\Theta_{\rm D} = 327\,{\rm K}$) and $CuGeO_3$ ($\beta_1 = 0.3\,{\rm mJ/mol{\cdot}K^4}$) [19–22].

Microscopic analysis and discussion. – To get more insight in the ordered phase, the knowledge of frustration and spatial anisotropy of the magnetic couplings is crucial. To estimate the main transfer integrals t and exchange couplings J, we performed full potential LDA band structure calculations using the FPLO code [23]. Cu $(3s, 3p, 4s, 4p, 3d)$, O $(2s, 2p, 3d)$ and Na $(2s, 2p, 3s, 3p, 3d)$ states were chosen as the basis set. Lower-lying states were treated as core states. The obtained bands near the Fermi energy $\varepsilon_{\rm F}$ are shown in fig. 4. Fitting them by an extended 3D tight-binding model we estimated the relevant t's (table I). From this fit we conclude that $NaCu_2O_2$ must be described by an exchange hierarchy: i) inchain and *ab*-plane (interchain); ii) bilayer, and iii) interbilayer ("double chain" in the notation of ref. [6]). The inchain dispersions along ΓY, UR, XS show deep minima in the middle of the

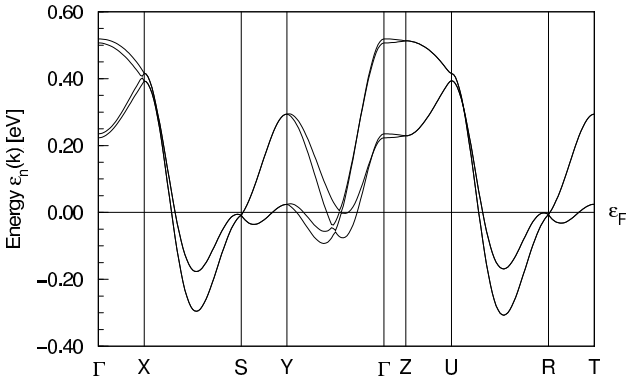

Fig. 4 – Band structure of $NaCu_2O_2$ near $\varepsilon_{\rm F}$, with $\Gamma = (0,0,0)$, X $= (1,0,0)$, Y $= (0,1,0)$, Z $= (0,0,1)$, R $= (1,1,1)$, S $= (1,1,0)$, T $= (0,1,1)$, U $= (1,0,1)$ in units of π/a, π/b, π/c, respectively.

TABLE I – *LDA-derived transfer integrals t and exchange couplings J. For notation see the right panel of fig.* 1 *and ref.* [4].

(meV)	y	$2y$	$3y$	$4y$	x	$\tilde{x}$	xy
$-t$	76.5	95.5	16	−2	73	11	25
J^{AFM}	6.9	10.7	0.3	0.005	7.1	0.1	0.8
J^{FM}	−11.4	−1.4	–	–	−1.4	–	–
J^{eff}	−4.5	9.3	0.3	~ 0	5.7	~ 0	0.8

BZ indicating a NNN transfer exceeding the NN term. This causes a sizable NNN superexchange and a strong inchain frustration. The effective exchanges J_{ij}^{eff}'s are given by the sum of AFM and FM terms [3]. The AFM contributions to any J estimated within a single-band Hubbard model are given by $J_{ij}^{\mathrm{AFM}} = 4t_{ij}^2/U$. For the screened on-site repulsion we used $U \approx \Delta_{pd} + 0.5\Delta_{pp} = 3.4\,\mathrm{eV}$, where Δ_{pd} and Δ_{pp} denote the differences of Cu and O on-site energies, respectively, which enter the five-band *pd* Hubbard model (see below). Comparing U with the calculated bare value $U_{\mathrm{b}} = 9.8\,\mathrm{eV}$ [3] using CuO_4 plaquette Wannier functions, an empirical local screening factor of 2.88 is obtained. Adopting also a screening length of 10 Å [2,24] the calculated NN bare FM part of −44 meV for J_y^{b} is reduced to −11.4 meV. Finally, summing the FM and AFM parts, we arrive at $J_y^{\mathrm{eff}} \approx -4.5$ meV. The NNN exchange $J_{2y} \approx +9.3\,\mathrm{meV}$ is dominated by the AFM superexchange as expected. The main interchain transfer process within the *ab*-plane t_{xy} is significantly smaller than the NN term t_y. The largest (diagonal) intrabilayer coupling $t_{\tilde{x}\tilde{y}} = 36\,\mathrm{meV}$ ($J_{\tilde{x}\tilde{y}} \sim 1.5\,\mathrm{meV}$) exceeds the inplane diagonal interchain and interbilayer couplings t_{xy} and $t_{\tilde{x}}$, respectively. Since the corresponding FM parts are expected to be smaller we ignored them. Thus, within LDA, we arrive also at $\alpha = J_2/|J_1| \approx 2$. The larger pitch $\phi = 82°$ compared with 62° for $LiCu_2O_2$ is plausible by the larger α [25]. Noteworthy, the interchain and DM exchange affect also the value of ϕ, but, in order to describe that ϕ within spin wave theory, long-range exchange J_3 and J_4 along $\boldsymbol{b}$ can be ignored in accord with an LDA analysis [26]. From this analysis we also conclude that $NaCu_2O_2$ is a much more pronounced quasi-1D spiral system (table I) compared with $LiCu_2O_2$ [3,4].

We performed also cluster calculations for Cu_nO_{2n} periodic chains (n = 3–6) within the frame of the five-band extended Hubbard model and mapped the low-lying multiplets onto ones of J_1-J_2 spin-1/2 Heisenberg rings. Starting from the parameter set proposed for Li_2CuO_2 [28], we first refined this set with respect to the isotropic O-hole distribution (inferred from O1*s* X-ray absorption and optical conductivity data [28, 29]) and to a proper evaluation of J_2. Changing slightly t_{pp} in chain direction and Δ_{pd}, we arrive at $\Delta_{pd} = 3.245$ and $\Delta_{pp} = +0.255\,\mathrm{eV}$ [30]. Thus a realistic Cu3*d*-O2*p* set mapping leads to nearly the same exchange integrals $J_1 = -4.12\,\mathrm{meV}$ and $J_2 = 7.79\,\mathrm{meV}$ as above.

Conclusions. – In conclusion, we propose a clear and consistent picture for the challenging low-temperature physics of $NaCu_2O_2$, a novel undoped chain cuprate. Below 13 K a sharp magnetic phase transition has been detected in specific heat and NMR data. The change of the ^{23}Na NMR lineshape reveals signatures of local magnetic fields caused by an inchain IC spin structure consistent with two weak FM conic spirals [31] alternatingly tilted from $\boldsymbol{c}$. Our picture relies on a well-founded combined analysis of various independent theoretical and experimental studies including phenomenological Heisenberg and microscopic *pd* Hubbard models and an extended tight binding analysis of LDA bands. The various approaches converge even quantitatively in finding the frustrated inchain NN and NNN exchange $-J_2/J_1 \approx 2$ as the main origin of the magnetic helix observed by NMR and neutron diffraction. Long-range exchange terms J_3 and J_4 are of minor relevance.

* * *

We thank D. IHLE, R. KUZIAN, U. RÖSSLER, A. N. BOGDANOV, M. BRADEN, R. KLINGELER, A. ZVYAGIN, and H. ESCHRIG for fruitful discussions. We appreciate the support provided by the grants CRDF RU-P1-2599-MO-04, RFBR 04-03-32876 (AAG) CRDF REC-005 (ASM), GIF 811-237.14 (JM, HR), the DFG (JM) and its Emmy-Noether-program (HR).

REFERENCES

[1] SCHOLLWÖCK U., RICHTER J., FARNELL D. J. J. and BISHOP R. F. (Editors), *Quantum Magnetism, Lect. Notes Phys.*, Vol. **645** (Springer, Berlin) 2004.
[2] ENDERLE M., MUKHERJEE C., FÅK B., *et al.*, *Europhys. Lett.*, **70** (2005) 237.
[3] GIPPIUS A. A. *et al.*, *Phys. Rev. B*, **70** (2004) 020406.
[4] DRECHSLER S.-L. *et al.*, *Phys. Rev. Lett.*, **94** (2005) 039705; *J. Magn. & Magn. Mater.*, **290** (2005) 345.
[5] CAPOGNA L., MAYR M., HORSCH P. *et al.*, *Phys. Rev. B*, **71** (2005) 140402.
[6] MASUDA T. *et al.*, *Phys. Rev. Lett.*, **92** (2004) 177201.
[7] BOGDANOV A. N. *et al.*, *Phys. Rev. B*, **66** (2002) 214410.
[8] TAMS G. and MÜLLER-BUSCHBAUM HK., *J. Alloy Compd.*, **189** (1992) 241: $c = 13.209$ Å.
[9] CHUNG E. M. L. *et al.*, *Phys. Rev. B*, **68** (2003) 14410.
[10] MORIYA T., in *Magnetism*, edited by RADO G. and SUHL H., Vol. **1** (Academic Press, N.Y.) 1963, p. 85.
[11] HÜCKER M. *et al.*, *Phys. Rev. B*, **70** (2004) 220507.
[12] From the mirror plane $\perp$ to the line connecting two NN (NNN) Cu positions along $\boldsymbol{b}$ (and bisecting it), it follows that $\boldsymbol{D}_i \|$ to that mirror plane, *i.e.* it should be within the *ac*-plane. From the twofold rotation axis containing the CuO_4 plaquette plane it follows that $\boldsymbol{D}_i \perp$ to the local CuO_4-plane.
[13] For a similar anisotropic up and downward shift of $T_c(H)$ of a magnetic IC-C transition in CuO see OTA S. B. *et al.*, *Phys. Rev. B*, **46** (1992) 11632.
[14] OSHIKAWA M. and AFFLECK I., *Phys. Rev. Lett.*, **79** (1997) 2886.
[15] BLINC R., *Phys. Rep.*, **79** (1981) 333.
[16] KOGOJ M., ŽUMER S. and BLINC R., *J. Phys. C*, **17** (1984) 2415.
[17] Our cluster approach fails in the infinite chain limit when the finite-size–related level spacing (spin gap) becomes comparable with k_BT. So 30 K is a low-T bound of our approach. The "suppression" of c_m below 30 K reflects the 3D crossover and subsequent magnetic ordering.
[18] JOHNSTON D. C. *et al.*, *Phys. Rev. B*, **61** (2001) 9558.
[19] MEIJER G. I. *et al.*, *Phys. Rev. B*, **58** (1998) 14452.
[20] HIRO Z. *et al.*, *J. Phys. Soc. Jpn.*, **69** (2000) 1824.
[21] LORENZ T. *et al.*, *Phys. Rev. B*, **56** (1997) R501.
[22] BRADEN M. *et al.*, *Phys. Rev. B*, **66** (2002) 214417.
[23] KOEPERNIK K. and ESCHRIG H., *Phys. Rev. B*, **59** (1999) 1743.
[24] HUBBARD J., *Phys. Rev. B*, **17** (1978) 494.
[25] BURSIL R. *et al.*, *J. Phys. C*, **7** (1996) 8605.
[26] The relevance of long-range exchange induced by antiadiabaticity cannot be excluded. Due to the missing knowledge of spin-phonon couplings and corresponding phonon modes it is impossible to evaluate it at present. However, adopting strong spin-phonon interaction $g \sim \mid J_1 \mid$ and soft phonon modes following ref. [27] one estimates a FM and negligible AFM corrections for J_3 and J_4, respectively, contrary to ref. [5] as well as slight renormalizations of J_1 and J_2.
[27] WEISSE A. *et al.*, *Phys. Rev. B*, **60** (1999) 6566.
[28] MIZUNO Y. *et al.*, *Phys. Rev. B*, **57** (1998) 5326.
[29] NEUDERT R. *et al.*, *Phys. Rev. B*, **60** (1999) 13 413.
[30] The change of sign (Δ_{pp}) compared with Li_2CuO_2 comes from the altered crystal field due to the NN chain in the adjacent bilayer and Cu^{1+} ions in the bilayer center.
[31] S. V. TJABLIKOV, *Methods in the Quantum Theory of Magnetism* (Plenum Press) 1967, fig. 6.